VOLUME 118, NUMBER 13
APRIL 3, 1996

JOURNAL OF THE AMERICAN CHEMICAL SOCIETY

Economy in Protein Design: Evolution of a Metal-Independent $\beta\beta\alpha$ Motif Based on the Zinc Finger Domains

Mary D. Struthers, Richard P. Cheng, and Barbara Imperiali*

Contribution from the Division of Chemistry and Chemical Engineering, California Institute of Technology, Pasadena, California 91125

Received November 29, 1995[⊗]

Abstract: An iterative design process involving the synthesis and structural analyses of five polypeptides patterned after the zinc finger domains is described. This process has led to the development of a metal-independent folded $\beta\beta\alpha$ motif, **BBA1**. In contrast to the zinc fingers and other naturally occurring peptides of similar size, this small monomeric structure folds without the assistance of metal cation ligation or disulfide bridges. To probe the effect of metal binding on the secondary and tertiary structure of peptides throughout the design process, a non-standard amino acid 3-(1,10-phenanthrol-2-yl)-L-alanine (Fen) was incorporated and its unique chromophore utilized for circular dichroism (CD) analysis. Advanced designs were analyzed by both CD and 2D NMR. The solution structure of **BBA1** was determined using NOE restrained simulated annealing. The average RMSD for the backbone atoms of residues 1−22 is 0.9 ± 0.3 Å. Analysis of the resulting structure reveals that the α-helix and β-hairpin are associated *via* a well-defined hydrophobic core including several key hydrophobic residues. A key design feature of **BBA1** is the utilization of a type II′ reverse turn to promote β-hairpin formation; a control peptide, in which the β-turn of **BBA1** was changed from a type II′ to a type II, lacks tertiary structure. Thus the effects of the turn type on the three-dimensional structure of this motif are dramatic. **BBA1**, a 23-residue mixed α/β motif, defines a new lower limit for the size of an independently folded polypeptide with native structure.

I. Introduction

The protein architecture exhibits remarkable structural and functional diversity and therefore represents an enticing target for synthetic manipulation. Crucial to the *de novo* design of functional polypeptides based on this architecture is the availability of synthetic motifs with defined tertiary structure. For this reason, considerable research in recent years has focused on the design of specific peptide sequences targeted to adopt a predictable three-dimensional structure.[1−6] In general, the most successful designs are either large (>60 residues)[7,8] or multimeric,[2,9−11] and many require either disulfide bridges[9,10,12] or metal ligation.[13−15] Our research in this field has focused on the assembly of small peptidyl motifs (<30 residues) which

[⊗] Abstract published in *Advance ACS Abstracts*, March 15, 1996.

(1) Regan, L.; DeGrado, W. F. *Science* **1988**, *241*, 976−978.
(2) Osterhout, J. J.; Handel, T.; Na, G.; Toumadje, A.; Long, R. C.; Connolly, P. J.; Hoch, J. C.; Johnson, W. C., Jr.; Live, D.; DeGrado, W. F. *J. Am. Chem. Soc.* **1992**, *114*, 331−337.
(3) Hecht, M. H. *Proc. Natl. Acad. Sci. U.S.A.* **1994**, *91*, 8729−8730.
(4) Betz, S. F.; Raleigh, D. P.; DeGrado, W. F. *Curr. Opin. Struct. Biol.* **1993**, *3*, 601−610.
(5) Fezoui, Y.; Weaver, D. L.; Osterhout, J. J. *J. Proc. Natl. Acad. Sci. U.S.A.* **1994**, *91*, 3675−3679.
(6) Raleigh, D. P.; Betz, S. F.; DeGrado, W. F. *J. Am. Chem. Soc.* **1995**, *117*, 7558−7559.
(7) Smith, D. D. S.; Pratt, K. A.; Sumner, I. G.; Henneke, C. M. *Protein Eng.* **1995**, *8*, 13−20.
(8) Pessi, A.; Bianchi, E.; Crameri, A.; Venturini, S.; Tramontano, A.; Sollazzo, M. *Nature* **1993**, *362*, 367−369.
(9) Quinn, T. P.; Tweedy, N. B.; Williams, R. W.; Richardson, J. S.; Richardson, D. C. *Proc. Natl. Acad. Sci. U.S.A.* **1994**, *91*, 8747−8751.
(10) Yan, Y. B.; Erickson, B. W. *Protein Science* **1994**, *3*, 1069−1073.
(11) Lovejoy, B.; Choe, S.; Cascio, D.; McRorie, D. K.; DeGrado, W. F.; Eisenberg, D. *Science* **1993**, *259*, 1288−1293.
(12) Kuroda, Y. *Protein Eng.* **1995**, *8*, 97−101.
(13) Handel, T. M.; Williams, S. A.; DeGrado, W. F. *Science* **1993**, *261*, 879−885.
(14) Lieberman, M.; Sasaki, T. *J. Am. Chem. Soc.* **1991**, *113*, 1470−1471.
(15) Ghadiri, M. R.; Soares, C.; Choi, C. *J. Am. Chem. Soc.* **1992**, *114*, 4000−4002.

0002-7863/96/1518-3073$12.00/0

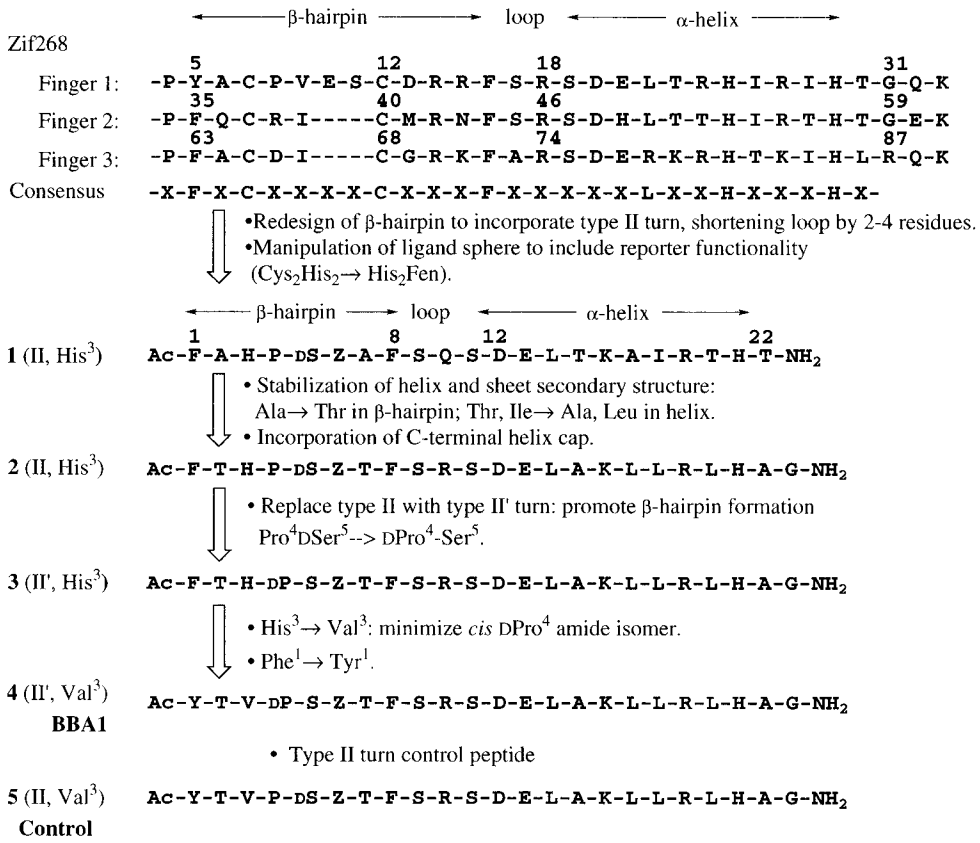

Figure 1. The design evolution of **BBA1**. The consensus zinc finger sequence[17] and that of Zif268, a DNA binding protein consisting of three domains which has been co-crystallized with DNA, are shown for comparison.[24] (Standard one-letter abbreviations for natural amino acids; Z = Fen.)

can afford versatile templates for elaboration into functional constructs. In order to achieve this ultimate goal the motifs should be compact, soluble, and monomeric. Consequently we have chosen to base our designs on independently folded natural polypeptides or protein domains, which display these desired properties. Natural polypeptides of this limited size and defined tertiary structure generally require either disulfides or metal binding sites for stability. We have therefore introduced a powerful approach for the manipulation of these natural systems to produce structurally related motifs that fold in the absence of such cross-linking agents.[16] A key feature of this approach is the exploitation of β-turns as structural nucleation elements to compensate for the stability originally afforded by cross-links. The $\beta\beta\alpha$ motif, exemplified by the zinc finger domains, represents an ideal initial target. Natural zinc finger peptides are small independently folded domains, which incorporate conserved hydrophobic residues (typically Tyr, Phe, and Leu),[17,18] and adopt defined solution structures *only* in the presence of specific metal cations.[19−21] This paper reports the design evolution of a metal independent $\beta\beta\alpha$ motif based on these peptides.

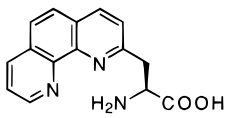

Fen

A number of biophysical tools can be employed for the analysis of peptide structure during the iterative design process. The circular dichroism (CD) signature of natural zinc fingers is well-known,[21,22] and served as a basis for the analysis of early designs. Furthermore, the limited size of the target polypeptides permits the incorporation of natural and synthetic amino acids. Nonstandard residues can be used both to control structure and to integrate functionality in order to monitor design progress. In this context, we have included the unnatural metal binding amino acid, 3-(1,10-phenanthrol-2-yl)-L-alanine (Fen),[23] to function as a reporter group. The phenanthroline chromophore of this residue exhibits a CD signal in the near-UV region upon metal binding provided that this moiety experiences a chiral environment. Therefore spectroscopic studies of peptides containing the Fen residue provide additional information on the effect of metal binding on structure. Most importantly, the small size of the target motif makes these constructs amenable to a rigorous structural characterization using ^{1}H 2D NMR techniques.

II. Results

Through the iterative design and analysis procedure outlined in Figure 1, five sequences based on the consensus zinc finger

(16) Struthers, M. D.; Cheng, R. P.; Imperiali, B. *Science* **1996**, *271*, 342−345.
(17) Berg, J. M. *Annu. Rev. Biophys. Biophys. Chem.* **1990**, *19*, 405−421.
(18) Michael, S. F.; Kilfoil, V. J.; Schmidt, M. H.; Amann, B. T.; Berg, J. M. *Proc. Natl. Acad. Sci. U.S.A.* **1992**, *89*, 4796−4800.
(19) Eis, P. S.; Lakowicz, J. R. *Biochemistry* **1993**, *32*, 7981−7993.
(20) Frankel, A. D.; Berg, J. M.; Pabo, C. O. *Proc. Natl. Acad. Sci. U.S.A.* **1987**, *84*, 4841−4845.
(21) Parraga, G.; Horvath, S. J.; Eisen, A.; Taylor, W. E.; Hood, L.; Young, E. T.; Klevit, R. E. *Science* **1988**, *241*, 1489−1492.
(22) Weiss, M. A.; Keutmann, H. T. *Biochemistry* **1990**, *29*, 9808−9813.
(23) The synthesis of N^{α}-fluorenylcarboxymethyl-3-(1,10-phenanthrol-2-yl)-L-alanine (Fmoc-Fen) has previously been reported: Fisher, S. L.; Imperiali, B. 33rd National Organic Symposium, **1993**.

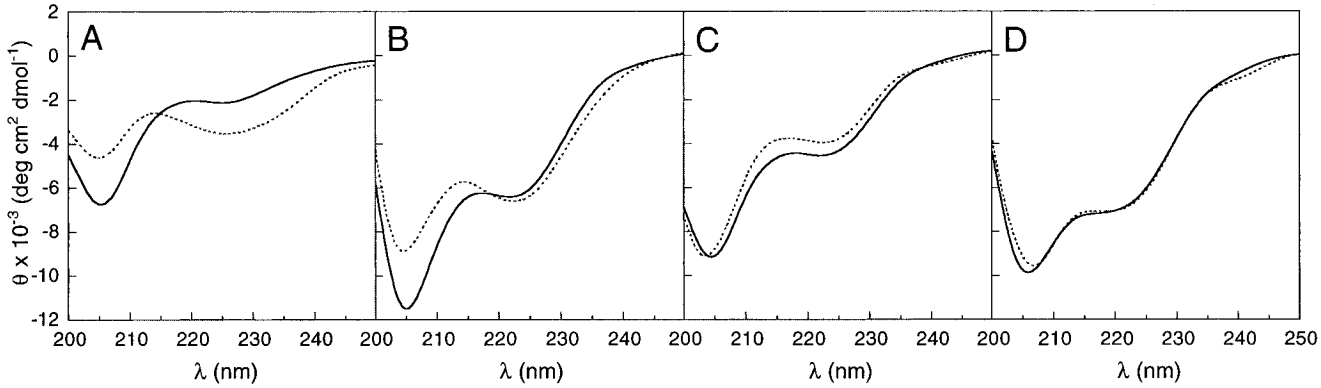

Figure 2. CD spectra of the intermediates in the design process: **A**, **1** (II, His^3); **B**, **2** (II, His^3); **C**, **3** (II′, His^3); **D**, **4** (II′, Val^3) or **BBA1**. The solid line represents the peptide spectrum in the absence of metal, the dashed line is the spectrum after the addition of Zn^{2+}. The 200−250-nm region reflects the secondary structure of each peptide. Each spectrum is normalized to the mean residue ellipticity.

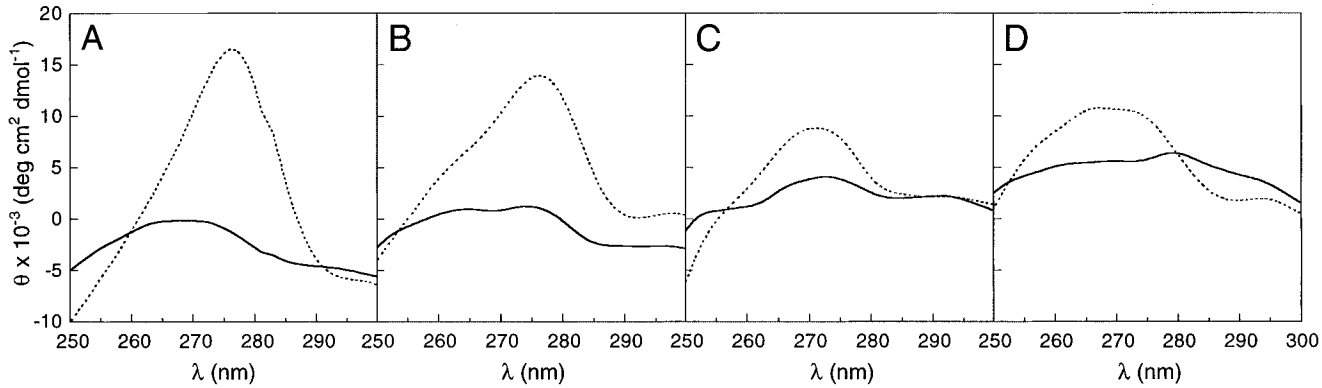

Figure 3. The near-UV region of the CD spectra of intermediates in the design process: **A**, **1** (II, His^3); **B**, **2** (II, His^3); **C**, **3** (II′, His^3); **D**, **4** (II′, Val^3) or **BBA1**. The solid line represents the peptide spectrum in the absence of metal; the dashed line is the spectrum after the addition of Zn^{2+}. CD signal in the 250−300 nm region results from the phenanthroline chromophore of the Fen residue. The spectra are normalized to the concentration of the phenanthroline chromophore.

sequence[17] and Zif268[24] were investigated. In the first generation peptide, **1** (II, His^3), the β-hairpin of the natural system was redesigned to incorporate a type II reverse turn, and the metal coordination sphere modified to include the Fen residue. (Each design is designated by its number followed by the turn type (II or II′) and the identity of the residue at position 3.) Amino acids with strong β-sheet (Thr, Val) and α-helix (Ala, Leu) propensities[25] were used to increase the inherent secondary structure in the second generation peptide, **2** (II, His^3). The utilization of a type II′ β-turn was investigated in the third generation peptide, **3** (II′, His^3). Analysis of this peptide by NMR revealed the presence of slowly interconverting *cis*−*trans* proline isomers, which was further investigated in a series of short peptides. Based on these studies, replacement of the residue at position 3 of the motif remediated this problem in the fourth generation design, **4** (II′ Val^3). The fifth generation peptide, **5** (II, Val^3), served as a control to probe the explicit role of turn type (type II vs type II′) in the establishment of defined secondary and tertiary structure.

Conformational Analysis of Peptides in the Design Process. (a) 1 (II, His^3): Peptide **1** (II, His^3) maintained the hydrophobic core residues of the consensus sequence (Phe^1, Phe^8, and Leu^{14}), while including a type II turn (Pro^4-DSer^5)[26] and a modified metal coordination sphere (His^3, Fen^6, and His^{21}). CD spectroscopy was used to investigate the metal binding behavior of **1** (II, His^3). These studies indicated that the structure of **1** (II, His^3) was metal dependent (Figure 2A). While the CD signature of the peptide in the absence of metal was largely random coil,[27] the addition of Zn^{2+} increased the overall secondary structure. The resulting spectroscopic signature of the peptide−Zn^{2+} complex, although considerably weaker, is reminiscent of that of natural zinc fingers.[21,22,28] Furthermore, metal-binding titrations monitored using the UV signal of the phenanthroline chromophore demonstrated the formation of a 1:1 Zn^{2+}−**1** (II, His^3) complex (K_D = 0.65 ± 0.60 μM). Concurrent with the increase in secondary structure, the addition of Zn^{2+} also produced a significant CD signal in the near-UV (250−300 nm) region. This signal was indicative of the formation of a chiral metal complex involving the Fen residue (Figure 3A). The CD spectra of uncomplexed peptide **1** (II, His^3) were invariant with pH (4.0−7.0) and peptide concentration (14 μM−1.3 mM), demonstrating the absence of aggregation behavior.

(b) 2 (II, His^3): Peptide **2** (II, His^3) incorporated sequence changes designed to enhance appropriate secondary structure. CD studies revealed that the structure of **2** (II, His^3) was more preorganized than that of **1** (II, His^3). The increased negative ellipticity of this peptide at 222 nm was consistent with greater inherent helicity in the absence of metal (Figure 2B). Nevertheless, addition of metal resulted in spectral changes consistent with the formation of a more structured peptide. The formation of a 1:1 complex with Zn^{2+} was confirmed by UV−vis spectroscopy (K_D = 0.89 ± 0.36 μM). The CD signature was

(24) Pavletich, N. P.; Pabo, C. O. *Science* **1991**, *252*, 809−817.
(25) Fasman, G. D. In *The Development of the Prediction of Protein Structure*; Fasman, G. D.; Plenum Press: New York, 1989; pp 193−316.
(26) Imperiali, B.; Fisher, S. L.; Moats, R. A.; Prins, T. J. *J. Am. Chem. Soc.* **1992**, *114*, 3182.
(27) Johnson, W. C., Jr. *Proteins: Struct. Func. Gen.* **1990**, *7*, 205−214.
(28) Weiss, M. A.; Mason, K. A.; Dahl, C. E.; Keutmann, H. T. *Biochemistry* **1990**, *29*, 5660−5664.

Table 1. Conformational Analysis of Model Type II′ Tetrapeptides

peptide	% *trans*	NOEs[a]	$-\Delta\delta/\Delta T$(ppb/K) Xaa	Ser	Fen
VF1: Ac-Val-DPro-Ser-Fen-NH_2	94	1, 2, 3, 4, 5	9.36	8.03	3.52
TF1: Ac-Thr-DPro-Ser-Fen-NH_2	94	1, 2, 3, 5	8.18	9.51	3.59
AF1: Ac-Ala-DPro-Ser-Fen-NH_2	92	1, 2, 3, 5	9.10	8.83	4.53

[a] NOEs present in ROESY experiment for the *trans* conformation. NOE identities are as presented in Figure 4.

not dependent on peptide concentration (15 μM−1.5 mM) or pH (4.0−8.1). Appearance of a distinct CD signal in the near-UV range (250−350 nm) upon addition of Zn^{2+} indicated the formation of a chiral complex involving the Fen, residue similar to peptide **1** (II, His^3) (Figure 3B).

(c) 3 (II′, His^3): The sequence of peptide **3** (II′, His^3) was modified from that of **2** (II, His^3) to incorporate a type II′ β-turn. Uncomplexed peptide **3** (II′, His^3) exhibited a CD signature similar to that seen for peptide **2** (II, His^3). However, it was notable that this CD spectrum changed very little upon addition of Zn^{2+}, indicating that the secondary structure for **3** (II′, His^3) was not metal dependent (Figure 2C). As with previous designs, the CD spectrum in the absence of metal was invariant with changes in pH (pH 4.5−8.0) and peptide concentration (14 μM−1.4 mM). UV studies conducted in parallel confirmed metal binding by the Fen residue ($K_D = 0.99 \pm 0.73$ μM). However, examination of the Zn^{2+}-induced changes in the near-UV CD spectrum suggested that the structural changes encountered by the phenanthroline chromophore were less dramatic than those observed for peptides **1** and **2**.

Peptide **3** (II′, His^3) was further analyzed by 2D NMR spectroscopy in the absence of metal cations. Observation of more than 35 spin systems, rather than the 23 expected for this peptide in the analysis, revealed the presence of slowly interconverting conformers.[29] These additional spin systems greatly complicated the spectral analysis, precluding complete sequence specific assignment. Dual spin systems that exhibited vastly different chemical shifts were observed for residues in the β-hairpin region containing DPro[4]. In contrast, residues in the helical region (Leu^{14}-Gly^{23}) exhibited dual spin systems with nearly overlapping chemical shifts. These results suggested that the two conformers were the *cis*−*trans* isomers of the amide bond of DPro[4].

In order to examine this isomerism in greater detail, the peptide Ac-Thr-His-DPro-Ser-Fen-Thr-NH_2 (**HP3**) corresponding to the turn region of **3** (II′, His^3) was synthesized. In solution, **HP3** was present as an equilibrium mixture of two conformers. NMR analysis by rotating frame nuclear Overhauser spectroscopy (ROESY) enabled the spectroscopic assignment of the two conformers. Observation of $d_{\alpha\alpha}(His^3,DPro^4)$ and $d_{\alpha\delta}(His^3,DPro^4)$ NOEs confirmed the identity of the *cis* (∼40%) and *trans* (∼60%) isomers, respectively.

In order to manipulate the *cis*−*trans* proline amide isomer ratio, a series of tetrapeptides was prepared. Since the nature of the residue immediately preceding proline has been shown to influence the proline amide geometry,[30,31] peptides containing the sequence DPro-LSer (positions $i + 1$ and $i + 2$, respectively) and various amino acids (Thr, Val, and Ala) at position (*i*) were synthesized and analyzed. The peptides studied are listed in Table 1. The *cis* amide bond between residue (*i*) and Pro ($i + 1$) results in a large downfield shift in the resonances for protons

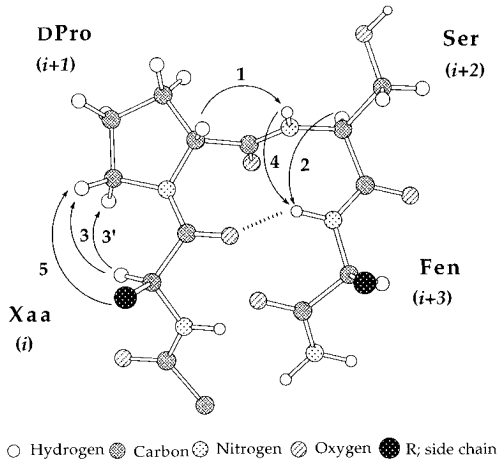

Figure 4. NOE interactions in the heterochiral type II′ reverse turn: **1**, $d_{\alpha N}$(Pro, Ser); **2**, $d_{\alpha N}$(Ser, Fen); **3** and **3′**, $d_{\alpha\delta}$(Xaa, Pro); **4**, d_{NN}(Ser, Fen); **S**, $d_{\beta\delta}$(Xaa, Pro). The (*i*)−(*i* + *1*) amide is shown in the *trans* conformation.

associated with residue (*i*). The *cis*−*trans* isomer ratio could therefore be quantified by integration of the 1D NMR signals of the methyl side chain protons of residue (*i*). The *trans* amide isomer dominated by greater than 90% for all sequences investigated. The peptides were further examined by ROESY and amide proton variable temperature (VT) NMR analyses to determine the propensity of each sequence to adopt a type II′ turn conformation in solution. The results of these studies are summarized in Table 1. The spectroscopic signature of type II′ turn formation includes the NOEs[32] illustrated in Figure 4 and a low VT coefficient ($-\Delta\delta/\Delta T$) for the Fen amide proton. In particular, NOE #4 [d_{NN} (Ser, Fen)] would be expected in the desired conformation. In the series of tetrapeptides studied, peptide **VF1** exhibited the lowest Fen amide temperature coefficient, as well as the NOEs characteristic of turn formation (Table 1). As a result of this study, the optimal turn sequence Val-DPro-Ser-Fen was included in the fourth generation design.

(d) 4 (II′, Val^3) (BBA1): Peptide **4** (II′, Val^3) (referred to hereafter as **BBA1**)[16] included the optimized type II′ turn and a $Phe^1 \rightarrow Tyr$ replacement to decrease NMR signal degeneracy. The proton resonances of the side chain of Tyr^1 in the *cis* and *trans* amide isomers of **BBA1** were sufficiently well-resolved in the 1D ^1H NMR spectra to allow quantification of the amide isomer ratio. Integration of these signals indicated <15% of the *cis* conformer.

The CD spectrum of **BBA1** strongly resembles that of the natural zinc fingers.[21,22] The addition of zinc results in only a slight change in the CD spectrum in the 190−250 nm range, indicating that secondary structure is metal *independent* (Figure 2D). In the first two designs, concomitant with the increase of the secondary structure upon addition of Zn^{2+}, a strong CD signal was observed in the near-UV region indicating the formation of a chiral Fen−metal complex. In contrast, for **BBA1**, a much weaker signal is observed, consistent with the idea that metal addition no longer dominates secondary and tertiary structure (Figure 3D). The formation of a 1:1 **BBA1**−Zn^{2+} complex ($K_D = 4.56 \pm 1.78$ μM) was confirmed by UV−vis spectroscopy. The CD spectrum of uncomplexed **BBA1**

(29) The identity and purity of peptide **3** (II′, His^3) was confirmed by mass spectral analysis (calcd MH^+ 2775.15, obsd MH^+ 2775.65) and capillary zone electrophoresis (CZE).

(30) Yao, J. Feher, V. A.; Espejo, B. F.; Reymond, M. T.; Wright, P. E.; Dyson, H. J. *J. Mol. Biol.* **1994**, *243*, 736−753.

(31) Grathwohl, C.; Wüthrich, K. *Biopolymers* **1976**, *15*, 2025−2041.

(32) Wüthrich, K. *NMR of Proteins and Nucleic Acids*; John Wiley and Sons: New York, 1986; p 292.

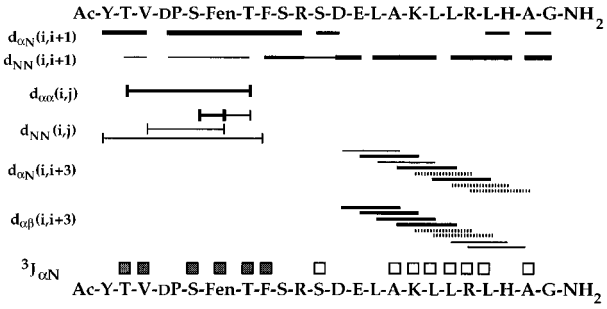

Figure 5. NOEs indicative of secondary structure in **BBA1** are illustrated in the diagram. The width of the lines represents the relative strength of the NOEs (200 ms NOESY), and a dashed line indicates that the NOE could not be identified due to overlap. Solid squares indicate $^3J_{\alpha N} > 8$ Hz, and open squares indicate $^3J_{\alpha N} < 6.8$ Hz.

was invariant with pH (4.5−8.5) and peptide concentration (8.2 μM−2.6 mM), indicating the absence of aggregation effects.[33]

The ^{1}H 2D NMR analysis of the uncomplexed peptide revealed the presence of well-defined secondary structure in good agreement with the design. NOEs indicative of helix formation ($d_{\alpha N}(i,i+3)$ and $d_{\alpha\beta}(i,i+3)$) were observed for residues 12−22. β-hairpin formation between residues 1 and 8 is indicated by a network of NOEs (Figure 5). Amide proton H/D exchange experiments conducted at pD* 4.5 (uncorrected) were also consistent with the desired β/α secondary structure.[16]

In addition to adopting the desired secondary structure, 2D NMR analysis indicates that **BBA1** folds with a defined tertiary structure. Specifically, long-range NOEs between protons of the side chains of residues Glu[13], Leu[14], Ala[15], Leu[17], and Leu[18] within the helix and residues Tyr[1], Val[3], Fen[6], and Phe[8] in the β-hairpin revealed the formation of a discrete hydrophobic core.[16] A portion of the 2D NOESY spectrum illustrating several of the diagnostic long-range NOEs is shown in Figure 6A. The solution structure of **BBA1** was solved through the use of NOE restrained simulated annealing (SA).[34] Forty-five structures were generated, 29 of which converged to a common fold. These 29 structures agree well with the intended design (Figure 7). The results of root mean squared analysis (RMSD) of these structures are summarized in Table 2.

Chemical and thermal denaturation experiments for **BBA1** were monitored by CD spectroscopy. The secondary structure of **BBA1**, as monitored at 222 nm, is rather stable and is only completely denatured in 8 M urea. Thermal denaturation does not appear to be complete, even at 80 °C (Figure 8).

(e) 5 (II, Val[3]): In order to further establish the importance of the type II′ β-turn in the successful generation of the metal-independent structure exhibited by **BBA1**, a control peptide was synthesized and analyzed. The turn type used in **BBA1**, a type II′, was replaced with a type II turn to produce peptide **5** (II, Val[3]). This peptide has an identical primary sequence to **BBA1**, differing only in the chirality of the central turn residues (Pro[4], Ser[5]).

The structure of peptide **5** (II, Val[3]) was evaluated in the absence of metal. NMR analysis of **5** (II, Val[3]) revealed that while the helical structure was largely maintained, both the β-hairpin and the tertiary structure observed in **BBA1** were absent. Several $d_{\alpha N}(i,i+3)$ and $d_{\alpha\beta}(i,i+3)$ NOEs, diagnostic of helical conformation, were present for residues 12−21 (Figure 9). In contrast, the NOEs that would be indicative of sheet

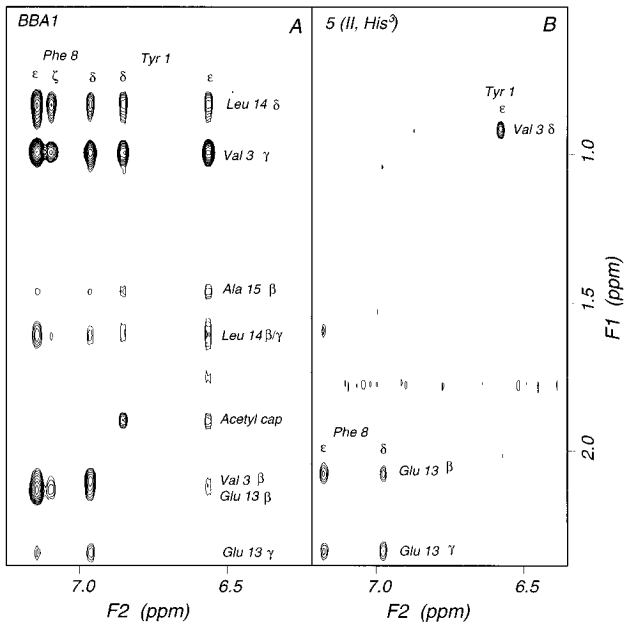

Figure 6. Identical regions of the NOESY spectra (300 ms mixing time) of **BBA1** (A) and **5** (II, Val[3]) (B) in D_2O. Long-range NOEs (for example Leu[14] δ protons to the ring protons (δ, ϵ, and ζ) of Phe[8] and Tyr[1]) are observed for **BBA1**. In contrast, very few NOEs are observed in the spectra of **5** (II, Val[3]).

formation were not observed. In addition, none of the NOEs diagnostic of tertiary structure were visible. Comparison of the identical regions of NOESY spectra of **5** (II, Val[3]) and **BBA1** underscore the contrasting structural behavior of the two peptides (Figure 6). This region contains a number of long-range NOEs of the aromatic side chain protons of Phe[8] and Tyr[1] with Leu[14]. Thus, although **5** (II, Val[3]) and **BBA1** differ only in the type of β-turn employed, the effects on secondary and tertiary structure are dramatic.

III. Discussion

Design Rationale. Polypeptides based on the zinc finger domains were evaluated for their ability to fold in the absence of metal (Figure 1). Conformational analysis was performed on five sequences, and the solution structure of **BBA1** (a metal-independent motif) was determined by NMR. The design was based on the sequences of the three fingers of Zif268[24] as well as the zinc finger consensus sequence.[17] In natural zinc finger peptides, an atypical loop connects the β-strands. In the crystal structure of Zif268, this loop appears to be flexible and poorly defined in the first finger.[24] A key feature of our design process was to delegate an active role to this part of the polypeptide sequence. Conformational studies of proteins and polypeptides have indicated that in some instances the β-turn may serve as a nucleating element in the folding process.[35−40] With this in mind, several recent computational[41−43] and spectroscopic

(33) Equilibrium centrifugation experiments performed on a closely related peptide differing only in the identity of the residue at position 1 (Tyr[1]→Phe[1]) confirmed that the peptide was predominantly monomeric in solution.

(34) Nilges, M.; Clore, G. M.; Gronenborn, A. M. *FEBS Lett.* **1988**, *239*, 129−136.

(35) Blanco, F. J.; Rivas, G.; Serrano, L. *Nature Struct. Biol.* **1994**, *1*, 584−590.

(36) Viguera, A. R.; Blanco, F. J.; Serrano, L. *J. Mol. Biol.* **1995**, *247*, 670−681.

(37) Stroup, A. N.; Gierasch, L. M. *Biochemistry* **1990**, *29*, 9765−9771.

(38) Montelione, G. T.; Arnold, E.; Meinwald, Y. C.; Stimson, E. R.; Denton, J. B.; Huang, S.-G.; Clardy, J.; Scheraga, H. A. *J. Am. Chem. Soc.* **1984**, *106*, 7946−7958.

(39) Wright, P. E.; Dyson, H. J.; Lerner, R. A. *Biochemistry* **1988**, *27*, 7167−7175.

(40) Blanco, F. J.; Jiménez, A.; Rico, M.; Santoro, J.; Herranz, J.; Nieto, J. L. *Eur. J. Biochem.* **1991**, *200*, 345−351.

(41) Yan, Y. B.; Erickson, B. W.; Tropsha, A. *J. Am. Chem. Soc.* **1995**, *117*, 7592−7599.

Table 2. Average RMSD Value (Å) of All 29 NMR Derived Structures from the Average Structure[a]

residues	RMSD backbone atoms	RMSD all heavy atoms
Tyr[1]-Ala[22]	0.9 (±0.3)	1.4 (±0.3)
all residues	1.2 (±0.5)	1.5 (±0.4)

[a] Standard deviations are in parentheses.

studies[26,44,45] have focused on establishing the stability of the various β-turn types. In particular, heterochiral type II turns have exhibited an inherent stability in theoretical and experimental investigations.[26,41,44] Thus, in the first generation design, **1** (II, His[3]), the β-hairpin region was engineered to incorporate a heterochiral type II β-turn forming sequence, Pro-DSer, while retaining only the two key conserved hydrophobic aromatic amino acids of the natural system at either end of the β-hairpin. It has been shown that with the exception of the metal binding ligands and the three highly conserved hydrophobic core residues (Phe[1], Phe[8], and Leu[14] in our system), alanine substitutions are tolerated at nearly every position in the natural zinc finger motif.[18] Therefore for the initial design, peptide **1** (II, His[3]), the central residues of the redesigned β-strands (positions 2 and 7) were alanines. The helix of **1** (II, His[3]) was based on the sequence of the Zif268 protein.[24]

The metal binding site of natural zinc fingers was also targeted for modification in the first generation design. For natural zinc fingers, assessment of divalent zinc coordination to the imidazole and thiolate ligands is complicated by the spectroscopically silent d^{10} Zn^{2+} ion.[47] Therefore, the elucidation of metal coordination for these motifs generally relies on observation of the tetrahedral coordination of Co^{2+} to these peptides.[20,48] This complex is spectroscopically observable because of the d−d transition of the peptide−Co^{2+} complex. Information on zinc binding is only determined indirectly by competitive titration of the Co^{2+} complex with Zn^{2+}.[48] To overcome this limitation and enable the facile assessment of metal binding properties for peptides generated during the design process, the metal coordination site of the natural zinc fingers was modified to include an unnatural bidentate amino acid (3-(1,10-phenanthrol-2-yl)-L-alanine (Fen)).[23] Monitoring the UV spectrum of the phenanthroline chromophore therefore allows the determination of metal binding affinities and stoichiometries for a variety of metals independent of coordination geometry. CD studies of the Fen moiety also allow the assessment of metal ion induced structural changes. The native Cys_2His_2 site was therefore converted to a His_2Fen site containing exclusively nitrogen-based ligands. This modification required the replacement of the two Cys ligands within the β-hairpin of Zif268 with His and Fen, respectively. The central histidine residue of the α-helix was replaced with alanine (position 17) to retain a four-coordinate site. The removal of the sulfhydryl-containing amino acids also eliminates the need for special handling techniques normally required to prevent the oxidation of these residues to the corresponding disulfide.[49] The first generation design exhibited a CD signature reminiscent of that found for natural zinc finger peptides[21,28] upon the addition of Zn^{2+}.

Towards the goal of a preorganized metal-independent structural motif, the second generation design, **2** (II, His[3]), included amino acid substitutions selected to increase inherent secondary structure.[25] The alanine residues in the β-hairpin region (positions 2 and 7) were replaced with the β-branched amino acid threonine, which has a higher propensity to adopt an extended or sheet-like conformation.[25] These positions are located on the solvent exposed exterior of the sheet and threonine also imparts hydrophilicity to this face. In addition, the β-branched amino acids in the α-helix were replaced with residues exhibiting high helical propensities (Leu or Ala), and the sequence was lengthened by one residue to include a glycine at the end of the helix. This residue is often found at the C-terminus of helices and is thought to serve as a helix "stop signal" or helix "cap".[50,51] The CD analysis of **2** (II, His[3]) indicated that this motif was considerably more preorganized than the first design, although the secondary structure was still metal dependent.

While the results of the CD studies of the second generation design were encouraging, it was evident that the structure of **2** (II, His[3]) required metal coordination. In order to address this issue, the third design targeted the β-hairpin region. Specifically the incorporation of a type II′ turn was investigated. Studies of the protein database[52] have found that tight β-hairpins include almost exclusively type I′ or type II′ β-turns, despite a general prevalence of type I and type II turns in protein structures.[53] Modeling studies performed with ideal turn and sheet dihedral angles focused on a structural comparison of the type II and type II′ turns.[54] The analysis revealed that a type II′ turn leads to convergent β-strands, while the more common type II turn affords divergent strands. Thus a type II′ turn might be more effective in promoting β-hairpin formation within the motif. The third generation design, **3** (II′, His[3]), incorporated a type II′ reverse turn.

The (ϕ, ψ) dihedral angles associated with the central two residues of the type II′ turn [(60°, −120°), (−80°, 0°)] are the inverse of those required for type II turn formation [(−60°, 120°), (80°, 0°)].[52] This fact leads to the opposite chirality preference for the type II′ turn compared to the type II turn. Specifically, the LPro[4]-DSer[5] sequence present in the first and second generation designs was replaced with DPro[4]-LSer[5] for **3** (II′, His[3]). While this peptide exhibited a CD spectrum that changed very little upon metal addition, a detailed structural analysis by NMR revealed the presence of approximately a 40/60 ratio of slowly interconverting *cis*−*trans* amide isomers of DPro[4]. This unexpected result highlights the importance of complementary CD and NMR studies in the analysis of designed polypeptides.

The design of the fourth peptide was based on an analysis of *cis*−*trans* proline isomerism in a series of tetrapeptides incorporating the type II′ β-turn. The optimal sequence, Val-DPro-Ser-Fen, was introduced in the turn region of peptide **4** (**BBA1**). Replacement of the residue immediately preceding proline

(42) Chalmers, D. K.; Marshall, G. R. *J. Am. Chem. Soc.* **1995**, *117*, 5927−5937.
(43) Yan, Y. B.; Tropsha, A.; Hermans, J.; Erickson, B. W. *Proc. Natl. Acad. Sci. U.S.A.* **1993**, *90*, 7898−7902.
(44) Aubry, A.; Cung, M. T.; Marraud, M. *J. Am. Chem. Soc.* **1985**, *107*, 7640−7647.
(45) Dyson, H. J.; Rance, M.; Houghten, R. A.; Lerner, R. A.; Wright, P. E. *J. Mol. Biol.* **1988**, *201*, 161−200.
(46) Lee, M. S.; Gippert, G. P.; Soman, K. V.; Case, D. A.; Wright, P. E. *Science* **1989**, *245*, 635−637.
(47) Maret, W.; Vallee, B. L. *Meth. Enzymol.* **1993**, *226*, 52−71.
(48) Berg, J. M.; Merkle, D. L. *J. Am. Chem. Soc.* **1989**, *111*, 3759−3761.
(49) Krizek, B. A.; Amann, B. T.; Kilfoil, V. J.; Merkle, D. L.; Berg, J. M. *J. Am. Chem. Soc.* **1991**, *113*, 4518−4523.
(50) Richardson, J. S.; Richardson, D. C. *Science* **1988**, *240*, 1648−1652.
(51) Presta, L. G.; Rose, G. D. *Science* **1988**, *240*, 1632−1641.
(52) Wilmot, C. M.; Thornton, J. M. *J. Mol. Biol.* **1988**, *203*, 221−232.
(53) Sibanda, B. L.; Thornton, J. M. *Nature* **1985**, *316*, 170−174.
(54) Antiparallel β-strands were generated using the dihedral angles $\phi = -139°$, $\psi = 135°$. A β-hairpin connecting these strands was created by adjusting the dihedrals of the central two-turn residues (type II: $\phi_1 = -60°$, $\psi_1 = 120°$; $\phi_2 = 80°$, $\psi_2 = 0°$; type II′: $\phi_1 = 60°$, $\psi_1 = -120°$; $\phi_2 = -80°$, $\psi_2 = 0°$).

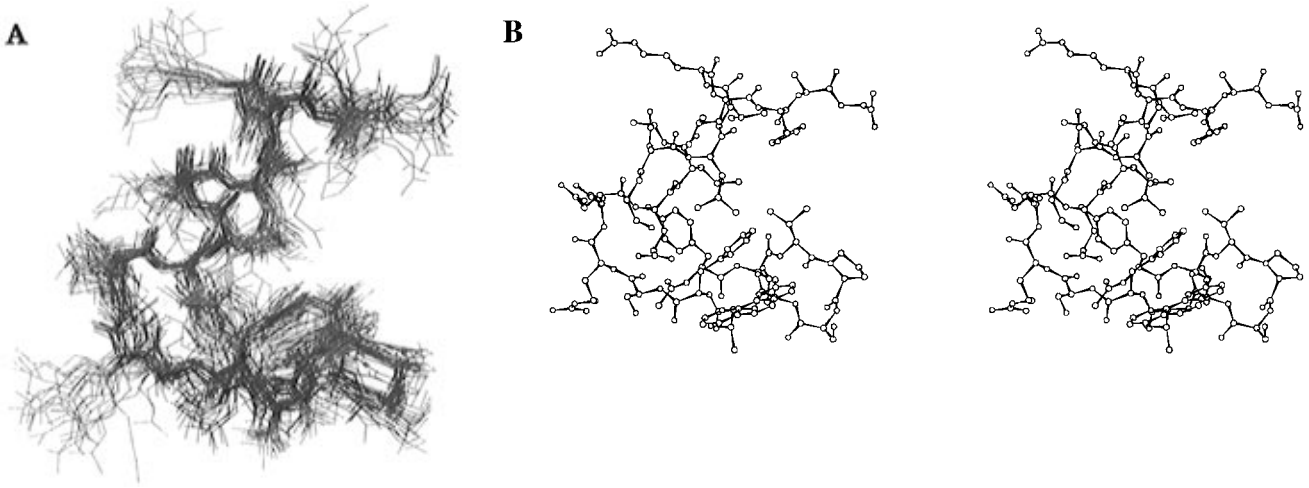

Figure 7. NMR derived structure of **BBA1**: (A) Overlay of the 29 NMR derived structures of **BBA1**; (B) stereo view of a representative NMR structure.

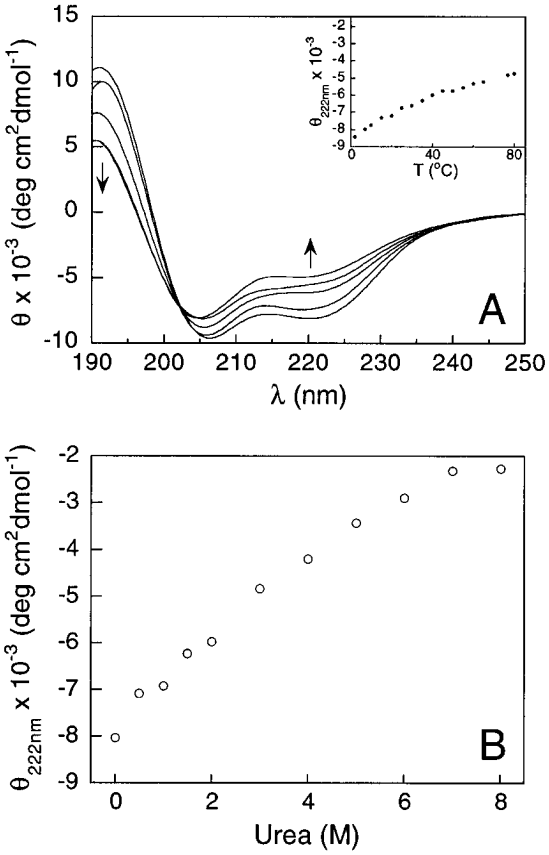

Figure 8. Chemical and thermal denaturation of **BBA1**: (A) The thermal denaturation of **BBA1** as monitored by CD. The CD spectra of **BBA1** at 7, 20, 40, and 80 °C are shown. The temperature dependence of the mean residue ellipticity at 222 nm is shown in the insert. (B) The dependence of mean residue ellipticity at 222 nm on urea concentration (0−8 M).

successfully limited the population of the *cis* proline amide isomer to less than 15%. In addition, the Phe at position 1 was replaced with tyrosine (commonly found at this position in natural zinc fingers) to avoid degeneracy in the NMR signals. CD studies indicated the formation of a metal-independent secondary structure. Detailed NMR analysis including the determination of the solution state structure by NOE-restrained simulated annealing (SA) confirmed that this peptide exhibited the desired three-dimensional architecture.

Structural Analysis of BBA1. The NMR analysis demonstrates that **BBA1** adopts a well-defined, monomeric tertiary

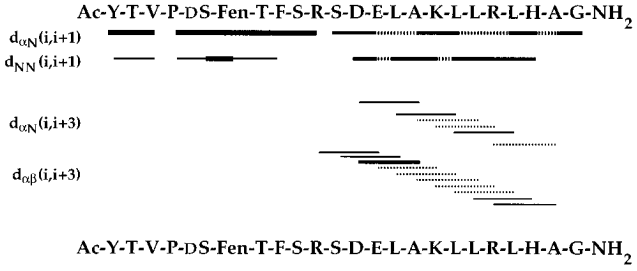

Figure 9. 2D NMR analysis of **5** (II, Val[3]). The width of the solid lines indicates the relative strength of the NOEs. The dashed lines indicate that the NOE could not be identified due to spectral overlap.

structure in aqueous solution. The 29 SA NMR structures generated for this peptide confirm that the α-helix and *β*-hairpin regions of the motif are in agreement with the intended design. Analysis of this ensemble reveals that 26 out of 29 structures (>90%) exhibit characteristic type II′ turn dihedral angles for DPro[4]-Ser[5]. The remaining three structures differed in the orientation of the central amide bond and did not conform to a defined turn type. Residues 13 through 20 adopt typical α-helix backbone dihedrals in most structures. Residues Asp[12] and His[21] appear to serve as "helix cap" residues.[51] The dihedral angles at these positions deviate significantly from ideal α-helix values ($\phi = -60°$, $\psi = -40°$) although these residues do participate in the expected 12(CO)→16(NH) and 17(CO)→21(NH) hydrogen bonds. In the same family of structures, it is apparent that the C-terminal glycine is considerably disordered, as are the side chains of surface-exposed residues such as Arg[10], Lys[16], and Arg[19]. While the latter is not surprising, the flexibility of the C-terminus can be addressed in future designs.

Although the NMR derived structure of **BBA1** resembles that of the natural zinc finger domains,[24,46] the designed motif is more "open" than its native counterpart. This observation is not surprising, since the metal center which cross-links the C-terminal end of the α-helix to the *β*-hairpin in the original system has been removed in our design.

Chemical and thermal denaturation experiments monitored by CD demonstrate that **BBA1** has considerable stability. The motif does not completely unfold even at temperatures as high as 80 °C and requires 8 M urea for complete denaturation. Comparable thermal stability has been observed with a metal-complexed natural zinc finger.[20] Although cooperative unfolding is often viewed as one of the hallmarks of native protein structure, noncooperative chemical denaturation has been observed for natural zinc fingers despite the presence of a well-

defined tertiary structure.[28] The unfolding studies employ CD spectroscopy which primarily measures the secondary and not the tertiary structure of the peptide. Therefore a peptide such as **BBA1**, which has been designed to possess a high degree of inherent secondary structure, might not be expected to manifest cooperative unfolding of secondary structure by this method. This is especially relevant for our system since the helix of **BBA1** is inherently stable in solution [as indicated by the NMR characterization of the control peptide **5** (II, Val^3)] and the CD signal is dominated by the helix signal.

Type II′ Turn as a Structural Nucleation Element. One of the key concepts presented in the design of **BBA1** was the use of a reverse turn as a structural nucleation element. Two different turn types (II and II′) were investigated for their ability to promote β-hairpin formation within the motif. The structural integrity of **BBA1** was attributed to the use of a type II′ β-turn. In order to confirm the explicit role of the turn in the final structure, a control peptide was synthesized in which the type II′ β-turn of **BBA1** was replaced with a type II β-turn. This peptide, **5** (II, Val^3), exhibits none of the NOEs indicative of β-hairpin formation which are present in **BBA1** (Figure 9). In addition, the long-range NOEs indicative of tertiary structure were absent. While both type II and type II′ β-turns exhibit inherent stability in aqueous solution as evidenced by spectroscopic studies of short model peptides,[26] the type II′ β-turn clearly has a greater ability to promote secondary and consequently tertiary structure in this system.

The β-turns have been extensively studied because of their structural and functional role in peptides and proteins. These structures have been shown to be critical in the bioactivity of small naturally occurring peptides and have been implicated in the process of protein folding.[55] This study highlights the potential of using these small motifs as structural nucleation elements in protein design. The use of the type II′ β-turn in concert with the judicious selection of amino acids to enhance inherent secondary structure has resulted in the successful design of a stable, well-defined $\beta\beta\alpha$ motif that folds in the absence of metal.

IV. Conclusions

The structure of small naturally occurring protein domains generally relies on either disulfide bridges or metal binding sites for stability.[56] Our goal has been the construction of stable polypeptide motifs based on natural systems, which are designed to fold in the absence of these cross-links. In our approach the utilization of appropriate structural nucleation elements compensates for the stability originally afforded by the cross-links. The success of this approach has been illustrated by the development of a metal-independent $\beta\beta\alpha$ motif, **BBA1**. While the $\beta\beta\alpha$ topology of **BBA1** is reminiscent of the zinc finger domains, elimination of the zinc binding site results in a more open structure. The absence of a metal-mediated cross-link creates an accessible cleft between the helix and the sheet which may be exploited as a small molecule substrate binding site in future designs. The template resulting from these efforts therefore provides a well-defined structural scaffold for the development of functional polypeptides.

(55) Rose, G. D.; Gierasch, L. M.; Smith, J. A. *Adv. Protein Chem.* **1985**, *37*, 1−109.

(56) While many peptides show significant secondary structure in water, formation of a well-defined tertiary structure in small polypeptides in the absence of cross-links is rare. Recently a limited report on the NMR analysis of a 33 amino acid polypeptide derived from the C-terminal domain of bovine rhodopsin indicated that a portion of this peptide adopts a compact structure: Yeagle, P. L.; Alderfer, J. L.; Albert, A. D. *Nature Struct. Biol.* **1995**, *2*, 832−834.

V. Experimental Details

Peptide Synthesis. The peptides were synthesized by solid phase methods using N^{α}-9-fluorenylmethyloxycarbonyl (Fmoc) amino acid pentafluorophenyl esters on a Milligen 9050 automated peptide synthesizer. Commercially available starting materials and reagents were purchased from Milligen Biosearch, EM Science, and Aldrich Chemical Co. Fmoc-PAL-PEG-PS resin (substitution 0.21 mmol/g) was used to afford C-terminal primary amides. The Fen residue was coupled off-line with 3 equiv of Fmoc-Fen (N^{α}-fluorenylcarboxymethyl-3-(1,10-phenanthrol-2-yl)-L-alanine) amino acid[23] and 4 equiv of 1-hydroxy-7-azabenzotriazole (HOAT) and *O*-(7-azabenzotriazol-1-yl)-1,1,3,3,-tetramethyluronium hexafluorophosphate (HATU)[57] and 8 equiv of diisopropylethylamine in *N*-methylpyrrolidinone for 2.5 h. Peptides were *N*-acylated on the resin using 7 equiv of acetic anhydride and 7 equiv of triethylamine in 3 mL of DMF for 2 h.

The peptides were deprotected and cleaved from the resin by treatment with Reagent K (trifluoroacetic acid/phenol/H_2O/thioanisole/ethanedithiol, 82.5:5:5:5:2.5)[58] for 2 h. Trituration with 1:1 ether/hexane afforded the crude peptide. The peptides were purified by reverse-phase HPLC on a C_{18} semipreparative column. Peptide purity was confirmed by analytical HPLC and capillary zone electrophoresis (CZE). Identity of all peptides was confirmed by MALDI or plasma desorption mass spectroscopy (PDMS). Peptide **1** MH^+ calcd 2635.9, obsd 2635.9 (PDMS). Peptide **2** MH^+ calcd 2775.2, obsd 2775.7 (PDMS). Peptide **3** MH^+ calcd 2775.2, obsd 2775.7 (MALDI). Peptide **4** MH^+ calcd 2753.1, obsd 2752.8 (MALDI). Peptide **5** MH^+ calcd 2753.1, obsd 2753.9 (MALDI).

Absorption Spectroscopy (UV−Vis) Studies. Absorption spectra were obtained on a Shimadzu UV-110 spectrophotometer using 1.0 cm path length quartz cuvettes. The concentrations of the peptide solutions were determined spectrophotometrically using the characteristic absorption band of the phenanthrolyl moiety ($\lambda_{max} = 268$ nm, $\epsilon_{max} = 20{,}890\ M^{-1}\ cm^{-1}$).[59] Aqueous solutions of known peptide concentrations (1−20 μM) were titrated with standardized metal cation solutions at room temperature in 0.05 M HEPES buffer at pH 8.25. The distinct red-shift of the phenanthrolyl $\pi-\pi^*$ transition upon metal chelation was monitored. The dissociation constants were determined by using the calculations outlined below. Data analysis was performed using KaleidaGraph version 3.0 (Abelbeck Software). A minimum of three titrations were performed for each peptide−metal cation complex. Binding isotherms were assumed to follow two-state equilibria; well-defined isosbestic points were observed in all cases. The dissociation constants (K_D) were obtained using an iterative process based on the Scott equation:[60]

$$\frac{b[M]}{\Delta A} = \frac{[M]}{[Pep]_t \Delta\epsilon} + \frac{K_D}{[Pep]_t \Delta\epsilon} \quad (1)$$

Where b = cell path length, [M] = free metal cation concentration, ΔA = change in absorbance due to complex formation, $[Pep]_t$ = total peptide in solution, and $\Delta\epsilon$ = change in molar absorptivity due to complex formation.

The dissociation constants (K_D) were calculated from plots of [M] vs [M]/ΔA by the following equation:

$$K_D = y\text{-intercept/slope} \quad (2)$$

Initially, data were considered only at high $[M]_{tot}$ so that the approximation $[M]_{tot} \approx [M]$ could be used. The resultant values of K_D and $\Delta\epsilon$ obtained by least-squared analysis were fitted to absorbances using eq

(57) Carpino, L. A.; El-Faham, A.; Minor, C. A.; Albericio, F. *J. Chem. Soc., Chem. Commun.* **1994**, 201−203.

(58) King, D. S.; Fields, C. G.; Fields, G. B. *Int. J. Pept. Protein Res.* **1990**, *36*, 255−266.

(59) The extinction coefficient for Fen previously reported ($\epsilon_{268\ nm} = 13950\ M^{-1}\ cm^{-1}$)[16] was determined from the absorbance spectrum of an analytically weighed and dried peptide sample. More recently, quantitative amino acid analysis was used to determine the absolute concentration of a stock solution of a Fen-containing peptide to provide the extinction coefficient ($\epsilon_{268\ nm} = 20890\ M^{-1}\ cm^{-1}$) to greater accuracy.

(60) Connors, K. A. *Binding Constants: The Measurement of Molecular Complex Stability*; John Wiley and Sons: New York, 1987.

1 to obtain better estimates of [M]. This was repeated in an iterative manner until the values of K_D and $\Delta\epsilon$ converged.

Circular Dichroism Spectroscopy Studies. Circular dichroism spectra were recorded on a Jasco J600 circular dichroism spectrometer. The concentration of the peptide solutions was determined spectrophotometrically using the characteristic absorption band of the phenanthrolyl moiety. The spectra were processed using the Jasco J600 System Software, and subsequently analyzed using KaleidaGraph. Metal cation titrations were performed with peptide concentrations ranging from 13 to 170 μM in 0.01 M TRIS buffer (pH 8.25) in either a 1.0 cm or a 0.1 cm path length quartz cell. Aggregation properties were investigated with peptide concentrations ranging from 10 μM to 2.6 mM at pH 4.5 in cuvettes of appropriate path length.

Thermal denaturation experiments for **BBA1** were performed in a 0.01-cm cell with a peptide concentration of 458 μM, pH 4.5, 10 mM acetate buffer. The peptide sample was equilibrated for at least 10 min after reaching a stable temperature and spectra were acquired at 2.5 and 7 °C and from 10 to 80 °C in 5 deg intervals. Chemical denaturation experiments were performed at pH 4.5 (acetate buffer), in a 0.1 cm cell with a peptide concentration of 84 μM, and urea concentration of 0−8 M. Each sample was equilibrated for at least 45 min before the spectrum was acquired.

NMR Studies. Two-dimensional NMR spectroscopy of **HP3**, **VF1**, **AF1**, and **TF1** was performed on a Bruker Instruments AMX500 500 MHz spectrometer. Complete sequence specific assignments were accomplished using total correlation spectroscopy (TOCSY)[61] and rotating-frame nuclear Overhauser effect spectroscopy (ROESY).[62] The temperature dependence of amide proton shifts was determined between 7 and 37 °C, in 5° increments. In all cases the chemical shifts varied linearly with temperature.

Two-dimensional ^{1}H NMR spectra of **BBA1** and **5** (II, Val^3) were obtained in both 90% H_2O/10% D_2O (6.2 mM **5** (II, Val^3) and 6.9 mM **BBA1**) and 99.98% D_2O (5.9 mM **5** (II, Val^3) and 5.2 mM **BBA1**) at 7 °C on a Varian 600 MHz instrument. All spectra were collected at pH 4.5, or pD* 4.5 (uncorrected meter reading). Complete sequence specific assignments for backbone and side chain protons were determined using TOCSY (mixing time 70 ms),[61] double-quantum filtered correlation spectroscopy (DQF-COSY),[63] and nuclear Overhauser spectroscopy (NOESY).[32,64] NOESY spectra were obtained for **BBA1** in H_2O (50, 100, 200, and 300 ms mixing times) and in D_2O (100, 200, and 300 ms mixing times) and for **5** (II, Val^3) in H_2O (100, 200, and 300 ms mixing times) and in D_2O (300 ms mixing time). Suppression of the water signal was accomplished by presaturation during the relaxation delay (1.5 s). Processing and analysis of the spectra were done using Felix 2.3 software (Biosym Technologies, CA). The $^3J_{\alpha N}$ coupling constants for **BBA1** were obtained from cross-peak measurements in a DQF-COSY spectra acquired at 25 °C to minimized the line broadening observed at 7 °C.

Structure Determination. The structure of **BBA1** was determined using a simulated annealing protocol (SA).[16,34] Cross peaks in the NOESY spectra (H_2O and D_2O) were classified as strong, medium, weak, or very weak based on the integrated volumes (50, 100, and 200 ms mixing times for H_2O spectra, 100 and 200 ms mixing times for D_2O spectra). The volumes were fit to a linear relationship with mixing time and calibrated to volume measurements for cross peaks corresponding to known interproton distances. Each NOE category was assigned a distance range: strong (1.0−2.5 Å), medium (1.8−3.5 Å), weak (1.8−5.0 Å), and very weak (1.8−5.5 Å). A maximum force constant of 25 kcal mol^{-1} Å^{-2} was used for all NOE distance restraints. Pseudoatoms were used when necessary and standard corrections were applied to interproton distance restraints involving pseudoatoms.[32] The use of pseudoatoms resulted in the generation of 301 restraints from 367 NOE volume measurements. The *cis* conformation accounting for less than 15% of the total signal was visible in the NMR spectra. NOESY cross peaks attributable to this conformation were omitted for the generation of restraints. Dihedral restraints were included in the SA analysis to enforce *trans* geometry of the amide bond between Val^3 and DPro^4. Forty-five structures were generated, 29 of which converged to a common fold and were considered for further analysis. The remaining 16 structures had high energies and significant restraint violations.

Acknowledgment. This work was supported by NSF Grant CHE-910445, a Parsons Foundation predoctoral fellowship (to M.D.S.), an NIH traineeship to R.P.C., and a Camille and Henry Dreyfus Teacher Scholar Award (to B.I.). We gratefully acknowledge the Dorothy Chandler, Camilla Chandler Frost Laboratory in Biology at Caltech for use of the Varian Unity Plus 600 NMR spectrometer.

JA954014U

(61) Bax, A.; Davis, D. G. *J. Magn. Reson.* **1985**, *65*, 355−360.
(62) Bax, A.; Davis, D. G. *J. Magn. Reson.* **1985**, *63*, 207−213.
(63) Piantini, U. Sørensen, O. W.; Ernst, R. R. *J. Am. Chem. Soc.* **1982**, *104*, 6800−6801.
(64) States, D. J.; Haberkorn, R. A.; Ruben, D. J. *J. Magn. Reson.* **1982**, *48*, 286−292.